Izvestiya, Physics of the Solid Earth, Vol. 39, No. 7, 2003, pp. 568–579. Translated from Fizika Zemli, No. 7, 2003, pp. 35–47.

Spatiotemporal Variations of the *S* Wave Attenuation Field in the Source Zones of Large Earthquakes in the Tien Shan

Yu. F. Kopnichev and I. N. Sokolova

Schmidt United Institute of Physics of the Earth (UIPE), Russian Academy of Sciences, Bol'shaya Gruzinskaya ul. 10, Moscow, 123995 Russia

Received March 4, 2002

Abstract—Spatiotemporal variations in the structure of the *S* wave attenuation field in the Tien Shan source zones of 11 large earthquakes with magnitudes of 6.4 to 8.3 are examined. The coda characteristics are derived from records of the aftershocks of these events, as well as from records of weak earthquakes that occurred a long time (up to 280 years) after them. Attenuation in the source zones at depths of 50–220 km is shown to regularly decrease with the time elapsed after large earthquakes, with its concomitant increase in the lower crust. An interpretation of the observed effects in terms of mantle fluids rising into the crust through major deep fault zones is proposed. The fluid concentrations in the mantle roots of fault zones and the fluid ascent rates are estimated.

INTRODUCTION

Studies of temporal variations in various geophysical and geochemical fields related to large earthquakes have focused on relatively short-term variations (up to a few years in duration), which are of predictive significance [Sobolev, 1993]. On the other hand, little is known as yet about the variations in various fields over fairly long time intervals (many tens of years) after strong tectonic events.

This work is concerned with the temporal variations in the attenuation field structure of shear waves that were observed in source zones after 11 large earthquakes with magnitudes of 6.4 to 8.3 in the Tien Shan. It is essential that the attenuation of short-period *S* waves is very sensitive to the concentration of the liquid phase (partially molten material or fluids) along their raypaths. The effective quality factor Q_s in some lithospheric regions can vary within 1.5 to 2 orders of magnitude over distances of ~10 km [Aptikaeva and Kopnichev, 1993; Aptikaeva *et al.*, 1996; Kopnichev, 2000]. The only parameter comparable in sensitivity to the presence of the liquid phase with the *S* wave adsorption is the electrical conductivity of rocks [Berdichevsky *et al.*, 1996]. Analysis of this information provides qualitatively new constraints on geodynamic processes in the source zones of large earthquakes [Kopnichev *et al.*, 2000].

GEOLOGICAL AND GEOPHYSICAL CHARACTERIZATION OF THE REGION STUDIED

The study region includes a significant part of the Tien Shan between 70° and 81° E, as well as the Chu and Ili basins in the north and the northern termination of the Tarim massif in the southeast. The geosynclinal period in the evolution of the major portion of the Tien Shan ended in the end of Hercynian; the newly formed platform experienced only insignificant differentiated movements in the Mesozoic. From the end of the Late Paleogene, tectonic movements resumed, producing the Tien Shan Mountains [Krestnikov *et al.*, 1979].

Deep fault zones have played a very important role in the tectonic history of the Tien Shan throughout all of its evolutionary stages (Figs. 1, 2). They dissect the entire crust and penetrate the upper mantle, forming the natural boundaries between the largest structural units. Most of the large faults are reverse faults steeply dipping at angles of more than 70° [Krestnikov *et al.*, 1979]. The faults trend mainly along the Tien Shan (E and NE) strike. The largest fault trending across the Tien Shan strike is the Talas–Fergana fault (Fig. 1). Many fault zones are associated with anomalies of strong *S* wave attenuation in the lower crust and upper mantle [Kopnichev and Nurmagambetov, 1987].

The crustal thickness is 40–45 km in the Chu and Ili basins and increases to 55–60 km in the mountainous areas of the Tien Shan [Krestnikov *et al.*, 1984].

According to deep seismic sounding and tomographic analysis, the upper mantle beneath the Tien Shan is characterized by low *P* wave velocities [Roecker *et al.*, 1993].

The study region is one of the seismically most active areas of the Earth. Let it suffice to say that, during the last 110 years, three $M > 8.0$ earthquakes occurred here (Fig. 1; Table 1). Sources of strong ($M > 6.0$) earthquakes are mostly confined to large fault zones. The high level of seismicity and the fairly dense network of seismic stations, including digital ones, make the Tien Shan region a perfect site for studying

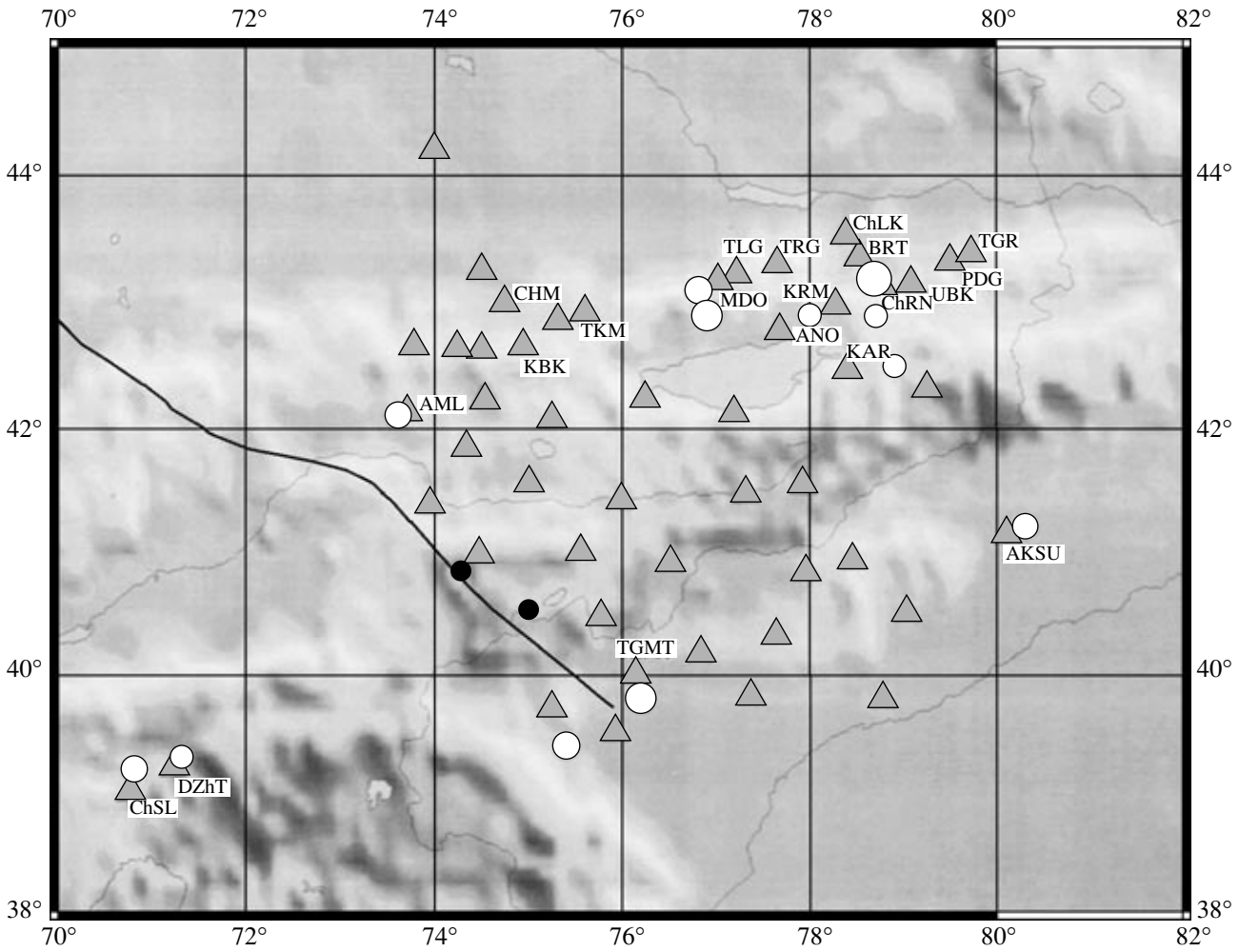

Fig. 1. Map of the study area. Open circles are epicenters of large earthquakes; larger sizes of the circles correspond to higher M values: $6.4 \le M < 7.0$; $7.0 \le M \le 8.0$; $M > 8.0$. Solid circles are springs with the highest (submantle) values of the He isotope ratio recorded in the Tien Shan. Triangles are seismic stations; names are given for stations mentioned in the text. The Talas–Fergana fault separating the western and central Tien Shan is shown.

the geodynamic processes related to large earthquakes.

DATA USED IN THE STUDY

We processed records obtained at 49 stationary and temporary seismic stations of the UIPE Integrated Seismological Expedition, the Institute of Seismology (MES, Kazakhstan), the Institute of Seismology (Academy of Sciences of Kyrgyzstan), and the Rensselaer Polytechnic Institute (NY, USA). The stations are equipped with short-period analog (SKM-3) and digital (PASSCAL) three-component arrays with passbands of 0.7–10 and 0.03–20 Hz, respectively. In addition, we analyzed seismograms obtained at analog frequency-selective seismic stations (FSSS) [Zapol'skii, 1971].

We examined seismograms of local earthquakes and quarry blasts at epicentral distances of up to 40–50 km. The energy classes K of these events varied within a range of 6–11 ($M \sim 1.0$–4.0). In all, a few hundred seismograms were processed.

We examined the coda characteristics in the source zones of 11 large earthquakes in the Tien Shan with magnitudes of 6.4 to 8.3, primarily in the area to the north of Lake Issyk-Kul (Figs. 1, 2; Table 1; with the exception of the Kashgar earthquake of August 23, 1985). Moreover, we used coda records obtained in the central and southern Tien Shan and in two zones of a high density of coseismic paleofractures in the northern Tien Shan (Figs. 1, 2).

METHOD

We used a method based on the analysis of envelopes of recorded short-period seismic coda. As previously established, the ~1-Hz coda is formed in Central Asia mainly by shear waves reflected from numerous subhorizontal boundaries in the crust and upper mantle

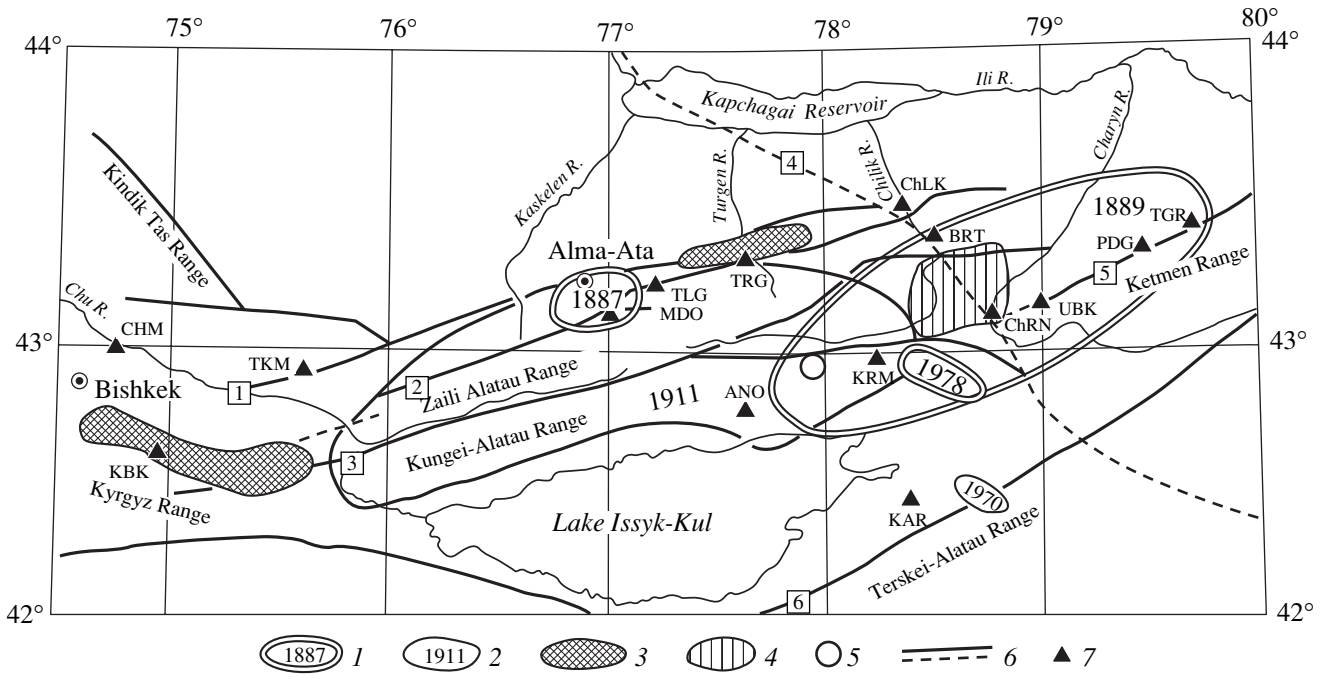

Fig. 2. Map showing the source zones of large earthquakes in the North Tien Shan: (*1*, *2*) isoseismal lines of large earthquakes at intensities of (*1*) 9 and (*2*) 8; (*3*) zones of high density of paleofractures; (*4*) weak attenuation area at depths of 50–220 km according to data from the ChRN station; (*5*) Baisorun earthquake epicenter; (*6*) fault zones (1, Alma-Ata; 2, Zaili; 3, Kemin–Chilik; 4, Kapchagai–Chilik; 5, Northern Ketmen; 6, Karakol); (*7*) seismic stations.

with minor velocity contrast [Kopnichev, 1985; Kaazik *et al.*, 1990; Aptikaeva and Kopnichev, 1993]. In this case, intervals of steep and gentle slopes in the envelopes are related, respectively, to regions of strong or weak attenuation of *S* waves in the lithosphere and asthenosphere.

Aptikaeva and Kopnichev [1993] showed that the strongest spatiotemporal variations in coda envelopes are observable at frequencies of about 1 Hz. Considering this, we compared them with the coda envelope characteristics obtained from records of the FSSS channel with a central frequency of 1.25 Hz. When broadband records of analog stations were used, they were preliminarily digitized at frequencies of 20 to 80 Hz with a wide scanner (or with an AVSI-6 apparatus when analyzing data gathered by magnetic recording stations ASS-6/12 Cherepakha).

Aptikaeva and Kopnichev [1993] established that, in the source zones of large earthquakes, coda envelopes can usually be divided into two groups, of relatively flat

Table 1. Parameters of large earthquakes in the Tien Shan

No.	Date	φ°, N	λ°, E	*h*, km	*M*	Locality
1	1716	41.2	80.3	30	7.5	Aksu
2	June 8, 1887	43.1	76.8	20	7.3	Vernyi
3	July 11, 1889	43.2	78.7	40	8.3	Chilik
4	Aug. 22, 1902	39.8	76.2	40	8.1	Kashgar
5	Jan. 3, 1911	42.9	76.9	25	8.2	Kemin
6	July 10, 1949	39.2	70.8	16	7.4	Khait
7	June 5, 1970	42.5	78.9	15	6.8	Sarykamysh
8	Mar. 24, 1978	42.9	78.7	30	6.8	Zhalanash–Tyup
9	Oct. 26, 1984	39.3	71.3	15	6.4	Dzhirgatal
10	Aug. 23, 1985	39.4	75.4	20	7.0	Kashgar
11	Nov. 12, 1990	42.9	78.0	20	6.4	Baisorun
12	Aug. 19, 1992	42.1	73.6	25	7.3	Suusamyr

and steeper slopes. An example of such envelopes that were constructed from records of early aftershocks of the Zhalanash-Tyup earthquake of March 24, 1978 ($M = 6.8$), obtained at the KRM station, is presented in Fig. 3. Two groups of envelopes markedly differing in slope are clearly distinguishable at $t < 60$ s (the time t is measured from the onset of radiation). After bringing into coincidence their $t = 60$ s levels, the $t = 16$ s amplitudes of one group are higher than those of the other by 0.60 logarithmic units.

Considering this fact and the previously established general patterns of the short-period coda in source zones [Kopnichev *et al.*, 2000], envelopes characterized by a weaker decay in the interval $t = 25$–100 s were selected for comparison from each zone. We examined the decay of envelopes separately in two intervals: 10–25 and 25–100 s. In accordance with the model interpreting the coda formation as a result of single *S* reflections [Kopnichev, 1985] and with an average focal depth set at about 10 km, the first interval corresponds to the middle and lower crust ($h \sim 20$–50 km) and the second corresponds predominantly to the upper mantle ($h \sim 50$–220 km).

The decay of envelopes in various areas was characterized by the effective quality factor Q_s; in the model of coda formation by single *S* reflections, the latter is given by

$$A(t) \sim \exp(-\pi t/Q_s T)/t, \qquad (1)$$

where T is the period of oscillations. Note that, in this case, Q_s includes the total contribution of attenuation and scattering effects, as well as reflections from relatively narrow fluid-saturated zones [Kopnichev, 1985; Kopnichev and Mikhailova, 2000].

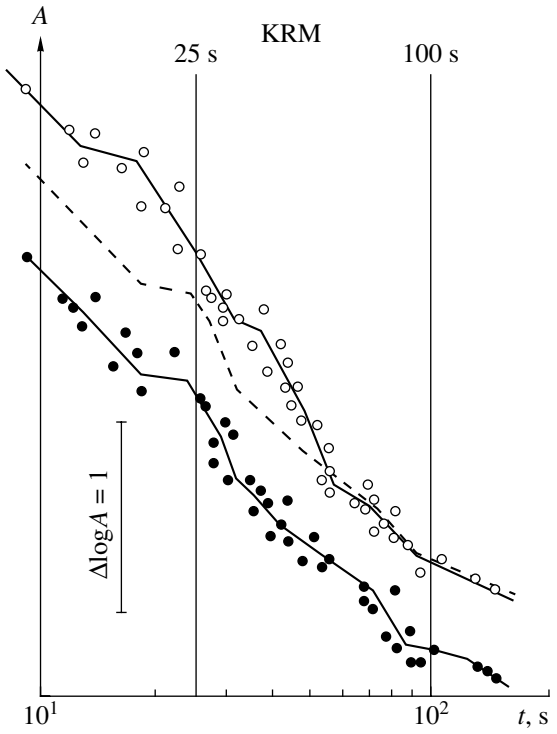

Fig. 3. Two types of coda envelopes from KRM records of early aftershocks of the Zhalanash-Tyup earthquake. The dashed line is the envelope with weaker decay in the time interval 25–100 s. Here and below, the 1.25-Hz FSSS channel is used.

ANALYSIS OF DATA

Coda characteristics from records of early aftershocks. Figure 4 presents examples of seismograms of two events recorded in the source zone of the Baisorun earthquake of November 12, 1990; these events occurred, respectively, 12 days and nearly nine years after the earthquake. At times of up to 60 s, the coda amplitudes of the first earthquake are seen to decrease much more rapidly.

Figure 5 shows the envelopes of records of weak events recorded in the source zones of four large earthquakes in the Tien Shan. For all four zones, we examined records of aftershocks that occurred within one or two months after the main shocks. In addition, the figure plots coda envelopes from records of aftershocks in three zones that occurred after comparatively long time intervals (up to 13 years) after these events.

The envelopes of the earliest aftershocks in the four source zones differ appreciably in shape. However, their common feature is long intervals of relatively rapid amplitude decay (approximately 15–100 s). Let t_b and t_e denote the respective times of the beginning and end of these intervals (Table 2).

As seen from Table 2, the t_b and t_e values vary within wide limits (respectively, from 18 to 55 s and from 50 to 105 s). The duration of these intervals tends to increase with magnitude. It is essential that, within the intervals of rapid amplitude decay, the Q_s values are relatively low (85–160) for the very first aftershocks of all earthquakes and markedly increase (to 240–320) with the time elapsing after these events.

Now, we examine the characteristics of coda envelopes in more detail. In 1992, the coda envelopes in the Suusamyr earthquake zone exhibited relatively rapid amplitude decay in the interval t = 55–105 s (with $Q_s = 160$). Seven years after this event, the shape of the envelopes appreciably changed. Most notably, the low Q_s range shifted into the interval t = 40–70 s, and very high Q_s values were observed at t = 70–95 s (Q_s increased from 140 to more than 2000).

The envelopes of events recorded in the Baisorun earthquake zone 9–10 years after the earthquake changed most in the interval 18–65 s (the quality factor increased from 85 to 320), whereas Q_s remained virtually unchanged in other time intervals.

A characteristic feature of the envelopes obtained from early aftershocks of the Zhalanash-Tyup earth-

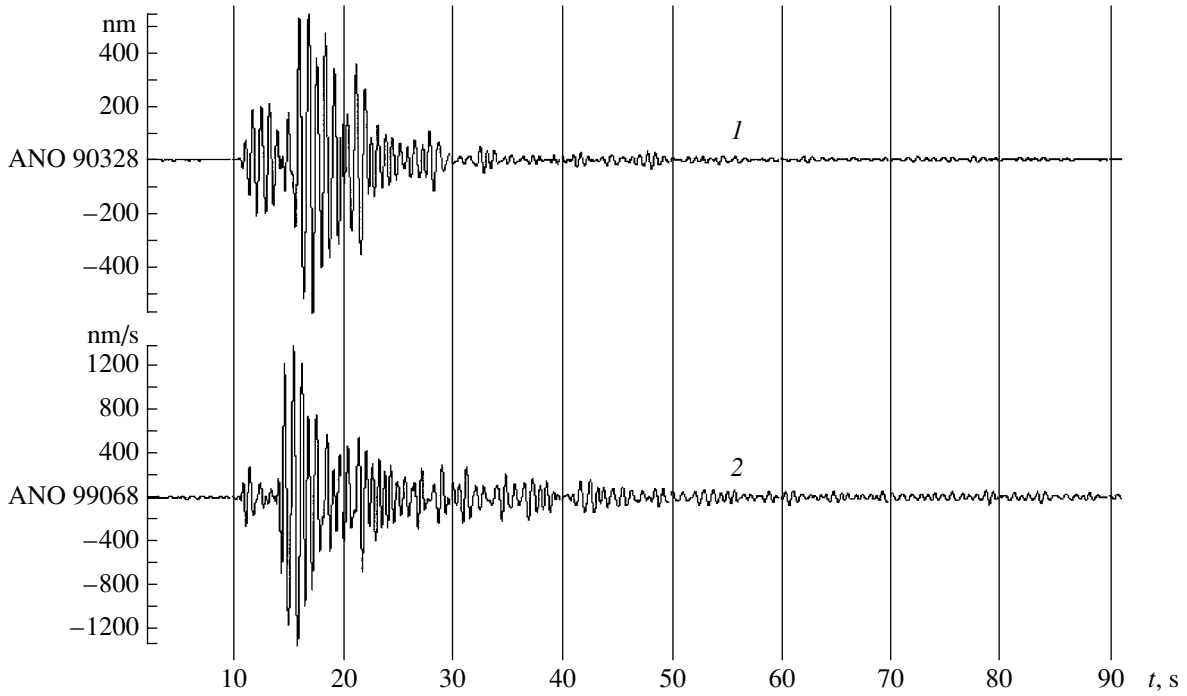

Fig. 4. Seismograms of weak events in the source zone of the Baisorun earthquake: (*1*) early aftershock of November 24, 1990 (43.00° N, 77.92° E; h = 5 km); (*2*) earthquake of March 9, 1999 (42.92° N, 77.83° E; h = 10 km).

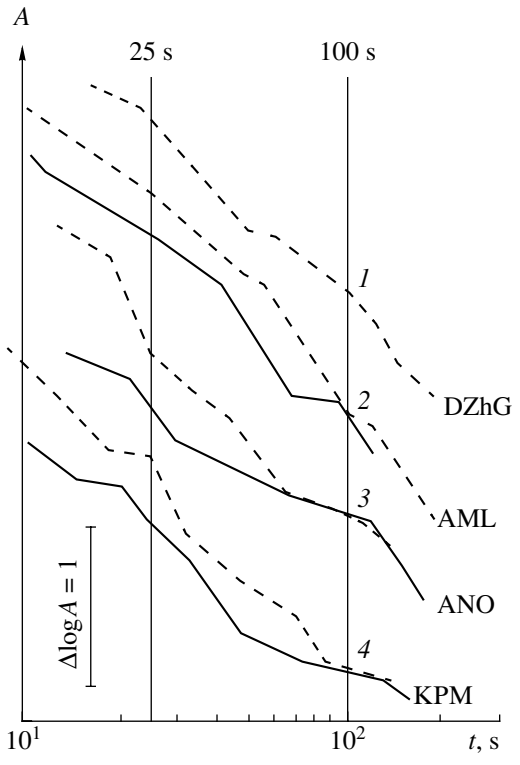

Fig. 5. Coda envelopes from records of events with epicenters in the source zones of large earthquakes (the dashed lines refer to early aftershocks). Earthquakes: (*1*) Dzhirgatal; (*2*) Suusamyr; (*3*) Baisorun; (*4*) Zhalanash-Tyup.

quake is the steep slope interval t = 24–85 s with Q_s = 140. 12–13 years after the earthquake, this interval had shifted to the values t = 20–45 s, with Q_s decreasing to 80. At the same time, the Q value abruptly increased at t = 45–90 s (Q_s > 2000).

Table 2 also gives the Q_s values in the interval 25–100 s. Strong attenuation (with Q_s varying from 170 to 300) is observed in the first few months after the large earthquakes in all four source zones. In seven years after the Suusamyr earthquake, the effective Q factor in this interval changed relatively little (from 180 to 250). Appreciable changes in the structure of the attenuation field took place in the Zhalanash-Tyup earthquake zone 12–13 years after the earthquake: Q_s increased to 370 (from 170 for the very first aftershocks). The Q_s values changed most dramatically 9–10 years after the Baisorun earthquake (from 300 to 2100).

Characteristics of coda envelopes observed long after large earthquakes. Figure 6 presents coda envelopes from five source zones of large earthquakes with $M \geq 7.3$ (the Aksu (1716), Vernyi (1887), Kashgar (1902), Kemin (1911), and Khait (1949) earthquakes; see Table 1). The envelopes are constructed from records obtained long after these events (respectively, more than 280, 100–110, about 100, nearly 90, and 30–40 years). On the whole, the decay rates of the envelopes are seen to be relatively high at t < 25 s and very low at t = 25–100 s. In the second interval, the minimum Q_s value is 700 in the Kemin earthquake zone and exceeds 2000 in three other source zones. (Note that the

Table 2. Characteristics of intervals of rapid amplitude decay in the coda of aftershock records

Earthquake	Years	Area of aftershocks		t_b	t_e	Q_s	Q_s (25–100 s)
		φ°, N	λ°, E				
Zhalanash-Tyup	1978	42.85–43.05	78.18–78.65	24	85	140	170
	1990–1991					320	370
Dzhirgatal	1984	39.20–39.32	71.25–71.40	24	50	105	275
Baisorun	1990	42.82–43.00	77.80–78.05	18	65	85	300
	1999–2000					320	2100
Suusamyr	1992	42.08–42.17	73.63–73.92	55	105	160	180
	1999					240	250

last value was chosen somewhat arbitrarily; actually, the Q_s factor in this case is formally equal to ∞ because the coda decays more slowly than according to the t^{-1} law, derived from the model of coda formation due to single reflections in the absence of attenuation.)

The spatial variations in the shape of coda envelopes were analyzed in more detail in the 1889 Chilik earthquake zone and its immediate vicinities. Figure 7 shows that, in the interval t = 25–100 s, the smallest envelope slope is observed in data of the ChRN station, located near the highest density zone of residual deformations due to the Chilik earthquake (Q_s > 2000). A slightly steeper slope of the envelopes was obtained from records of the PDG station, which is also located in the maximum intensity zone (Q_s > 1200). A very weak coda decay interval of 12–54 s is observable from records of the UBK station, located between the two aforementioned stations. However, the overall attenuation in the interval 10–100 s is much stronger here compared to the ChRN and PDG stations (Q_s = 205). Very strong attenuation is observable from records of the TGR, BRT, and ChLK stations, located near the boundary of the intensity-9 zone (in the interval 25–100 s, the Q_s values are 200, 240, and 210, respectively).

For comparison, Fig. 8 shows coda envelopes from records of events in zones of a high density of coseismic paleodeformations related to M > 6.5 earthquakes that occurred supposedly some 1000 years ago [Krestnikov *et al.*, 1979; Galperina *et al.*, 1985]. One of these zones lies to the east of the TLG station and the other is situated east of the city of Bishkek, to the south of the TKM station (Fig. 2). All envelopes exhibit a fairly rapid amplitude decrease, with Q_s varying from 190 to 235 in the interval 25–100 s.

Figure 9 presents the dependence of Q_s in the interval 25–100 s on the time ΔT that has elapsed after a large earthquake. The Q factor is seen to increase relatively slowly until $\Delta T \sim 10$ years (with the only exception being data for the Baisorun earthquake). Afterward, the Q_s increase rate markedly rises. The Q_s factor reaches a maximum 30–40 years after an earthquake and later remains virtually unchanged (the resolution of the method is insufficient for establishing any more subtle distinctions of the Q_s parameter).

Figure 10 also shows the scatter in the coda envelope data recorded in the Tien Shan source zones of nine large earthquakes long after these events (the least interval is 9–10 years, in the Baisorun earthquake zone); the envelopes were brought into coincidence at t = 100 s. The effective Q factor in this interval varies from 700 to ∞. The slope of the envelopes markedly

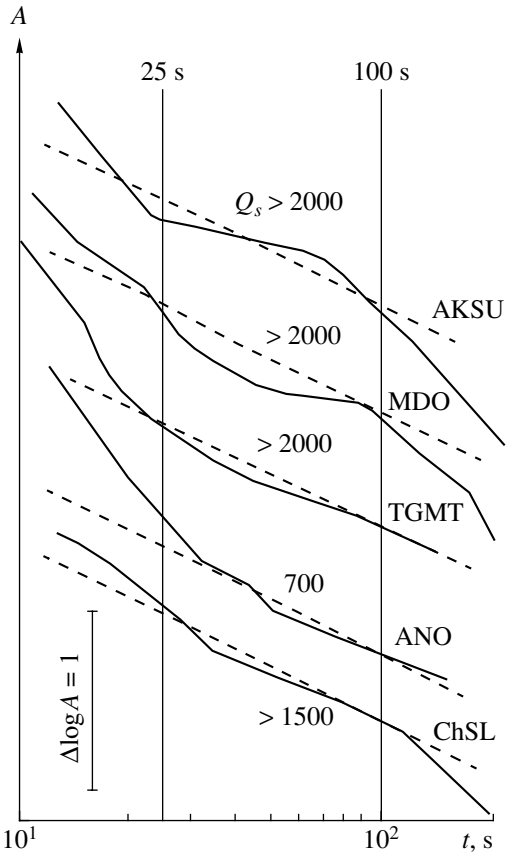

Fig. 6. Coda envelopes from events recorded long after large earthquakes. The dashed lines are the t^{-1} curves.

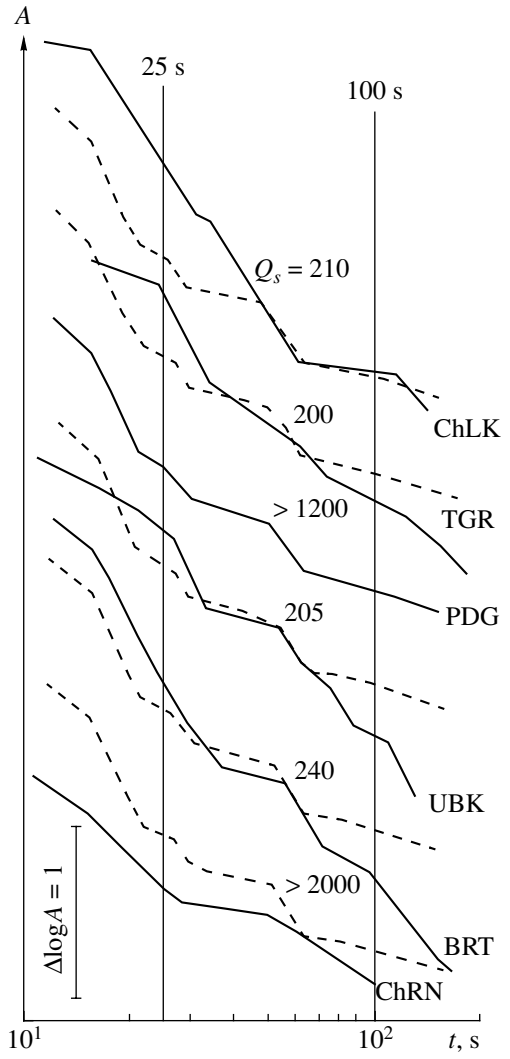

Fig. 7. Coda envelopes from records of stations located in and near the maximum intensity zone of the Chilik earthquake of 1889. The dashed lines are coda envelopes of the PDG station.

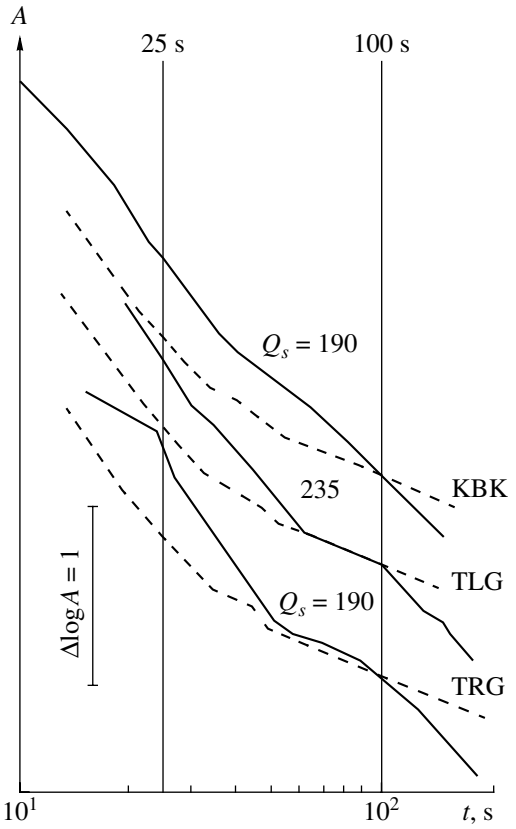

Fig. 8. Coda envelopes from records of earthquakes in zones of a high density of paleofractures in the North Tien Shan. The dashed lines are the coda envelopes from the source zone of the Kemin earthquake (the ANO station).

increases at $t < 25$ s (with Q_s varying mainly from 30 to 90).

In addition, Fig. 10 shows the scatter in the data for the coda envelopes derived from the records of 46 digital and analog stations installed in the central Tien Shan (Fig. 1). The data plotted in the figure relate to events whose epicenters are located in mountainous areas of the Tien Shan. Moreover, we excluded data from the source zones of the aforementioned large earthquakes with an anomalously weak coda decay. In this case, the envelopes decay much more rapidly in the range 25–100 s, with Q_s varying from 105 to 400.

For comparison, Fig. 11 presents the coda envelopes from records of earthquakes and explosions with epicenters in the areas of the large Issyk-Kul and Chu basins characterized by a very low seismicity level. The coda amplitudes in the interval 25–100 s are seen to decay more weakly compared to the mountainous areas, and Q_s varies from 560 (the KAR station) to 2100 (ANO). On the other hand, the CHM and ANO stations yield relatively steep slopes of envelopes at $t < 25$ s.

DISCUSSION

Factors responsible for the variations in the structure of the attenuation field. Our data indicate that the structure of the *S* wave attenuation field varies regularly with the time measured from a strong earthquake. As is well known, the attenuation of *S* waves can substantially decrease in the case of a marked decrease in the percentage of molten material or fluids in a given volume of the crust or upper mantle. As seen from Figs. 4, 5, and 9, noticeable variations in the structure of the attenuation field at depths of ~50–220 km are observable 7–10 years after an $M > 6.0$ earthquake. Attenuation field variations with even shorter periods were found to precede large earthquakes [Kopnichev and Sokolova, 1997; Kopnichev, 1997; Kopnichev and Mikhailova, 2000]. Evidently, such rapid (on the geological time scale) variations cannot be related to melting or crystallization processes in rocks. Hence, the

effects discovered can be attributed solely to active migration of fluids in the crust and upper mantle.

Spatiotemporal pattern of the fluid field. As is evident from Figs. 4 and 5, the concentration of fluids in source zones at depths of ~50–220 km is relatively high during the first few months after large earthquakes. A decrease in the attenuation at such depths with time indicates that the fluids gradually ascend from the upper mantle into the crust, in agreement with data on high attenuation at depths of ~20–50 km (Fig. 10).

Since the coda envelopes were constructed at times of $t > 10$ s, our data give no constraints on the variations in the attenuation field structure (and fluid ascent) at depths shallower than 15–17 km. However, available geochemical data on the presence of mantle isotopes of He and C in hydrothermal waters in source zones of large earthquakes [Asada *et al.*, 1984; Nikolaev *et al.*, 1992; Italiano *et al.*, 2001] are evidence of the ascent of juvenile fluids toward the Earth's surface. Note, in this context, that maximum values of the He isotope ratio in the Tien Shan region that had not been previously observed outside active volcanic areas [Polyak *et al.*, 1990] were discovered in the Talas–Fergana fault zone a few yeas after the $M = 7.0$ Kashgar earthquake of August 23, 1985, at distances as short as 100–200 km from its source (Fig. 1; Table 1). The ascent of deep fluids to the surface can also be indicated by a substantial increase in the total yield of springs in source zones after large earthquakes, particularly if their focal mechanisms are normal faults [Muir-Wood and King, 1993].

Magnetotelluric sounding (MTS) data suggest that fluid concentrations in the lower crust are relatively high, whereas the middle crust acts as a fluid-impermeable barrier [Kissin, 1996]. Available data show that large earthquakes can break the integrity of this barrier and, as a result, deep fluids start moving toward the Earth's surface through subvertical or inclined channels. Such channels are traceable in the crust from *S* wave attenuation [Kopnichev and Sokolova, 1997, 2001] and MTS [Berdichevsky *et al.*, 1996] data.

As seen from Figs. 3, 6, 7, and 10, most source zones of large earthquakes are characterized, within a long time after their occurrence, by a rapid coda decay in the interval 10–25 s, indicating very high *S* wave attenuation at depths of 20 to 50 km. This suggests that the major portion of mantle fluids does not reach the surface and remains in the lower crust. We should emphasize that additional fluid supply from the upper mantle removes the objections to the fluid model of the lower crust conductivity [Vanyan and Hyndman, 1996] advanced by some researchers who stated that, given a high hydrodynamic permeability of the middle crust, fluids in the lower crust should be exhausted within a geologically short time.

Note that mantle fluids can ascend even in low-seismicity areas as a result of intense anthropogenic activities, for example, the numerous high-yield nuclear explosions at the former Semipalatinsk Test Site [Kopnichev and Sokolova, 2001].

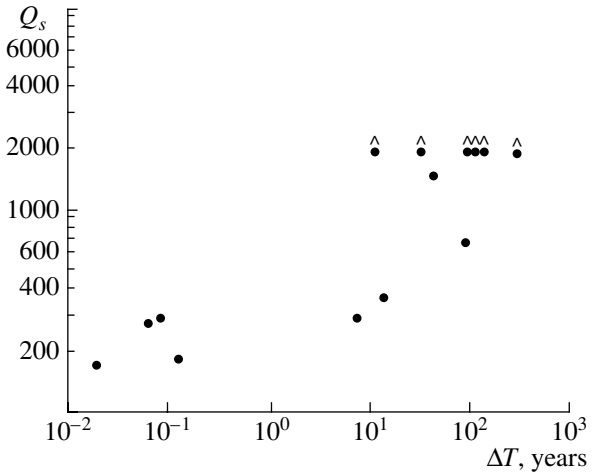

Fig. 9. Q_s versus ΔT. The capped dots are minimum estimates of Q_s.

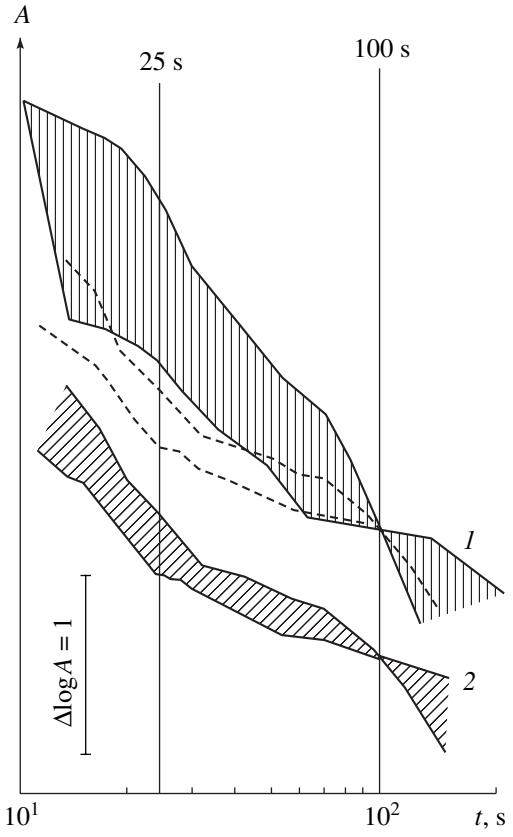

Fig. 10. Spread (*2*) of the coda envelope data from records of weak earthquakes in the source zones of nine large earthquakes in the Tien Shan (see Table 1, with the exception of the Dzhirgatal, Kashgar (1985), and Suusamyr earthquakes). (*1*) Scatter in the data from records of 46 stations in the Tien Shan region. The dashed lines show the spread of data (*2*).

The density of fluids being much lower compared to the solid skeleton, their ascent from the upper mantle

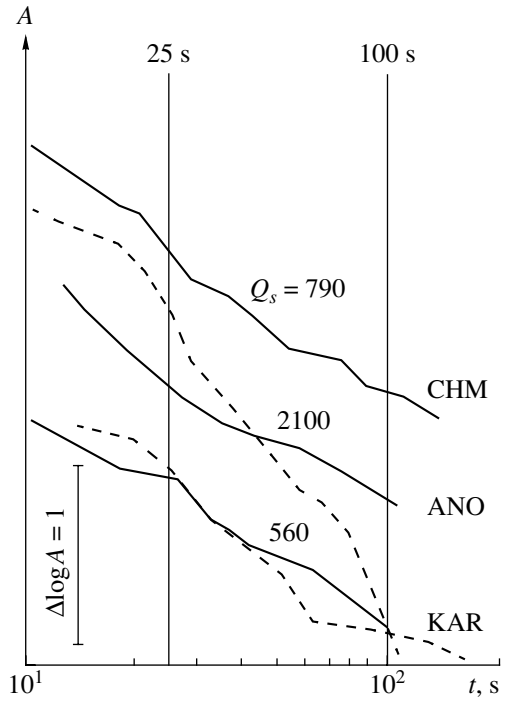

Fig. 11. Coda envelopes for epicenters in the Chu (CHM station) and Issyk-Kul basins. The dashed lines show the scatter in the data from mountainous areas (Fig. 10).

can be accompanied by a large energy release. Thus, we may state that an important effect of crustal earthquakes is the release of deep fluids, ultimately decreasing the Earth's potential energy. This energy is primarily expended on the heating of the lithosphere and on orogenesis.

As can be inferred from Fig. 7 and previous data [Aptikaeva and Kopnichev, 1993; Aptikaeva *et al.*, 1996], the structure of the attenuation field in source zones of earthquakes with $M > 6.5$ is highly inhomogeneous. As seen from Table 2, fluids in the Baisorun earthquake zone can ascend from a 20×20-km area comparable in size with the source zone. (Note that the size of the Fresnel zone for 1.25-Hz *S* waves reflected at a depth of about 200 km is ~20 km.)

Fluid ascent from depths of up to 220 km in the source zone of the Chilik earthquake may have occurred in the vicinities of the ChRN and PDG stations. The area of weak attenuation in the vicinity of the ChRN station is elongated from SW to NE; taking into account the refraction of reflected rays in the crust, its length is about 35 km. This area is bounded to the north, west, and east by zones of relatively strong attenuation near the BRT, KRM, and UBK stations. The attenuation is also strong in the areas of the ChLK and TGR stations, located near the boundary of the intensity-9 zone. Data of the KRM station suggest that, until 1978, fluids apparently did not rise from the upper mantle in the maximum intensity zone of the Zhalanash-Tyup earthquake, which lies entirely within the intensity-9 contour of the 1889 earthquake (Fig. 2).

It is important that fluids are likely to rise primarily through large fault zones or their intersections. This is well demonstrated by the case of the Chilik earthquake: the weakest attenuation is obtained from records of the ChRN station, located near the intersection of the Kapchagai–Chilik and Northern Ketmen fault zones. Previously, this fact was also established in the area of the TLG station, located at the intersection of the large regional Zaili fault and a transverse fault striking across the Tien Shan trend [Kopnichev and Sokolova, 1997; Kopnichev, 2001]. This conclusion agrees with the general pattern established by Rogozhin [2000]: the sources of large earthquakes are confined to junction and intersection areas of large faults. Note also that the majority of hydrothermal springs concentrate around junctions or terminations of faults [Curewitz and Karson, 1997].

Now, we mention some features of fluid migration in the upper mantle. As was pointed out by Letnikov [1992], "under upper mantle conditions, fluids possess unique properties such as an exceptionally high compressibility, very large energy and mass capacities, high geodynamic permeability, and the ability to create a pathway for fluid flow in a viscoelastic medium." These properties of mantle fluids substantially facilitate their ascent into the crust.

Results of experimental research on fluid convection indicate that ascending liquid flows concentrate in narrow zones, develop in an impulsive regime, and have velocities many times higher than those of diffusive percolation of fluids downward [Fyfe *et al.*, 1978]. This implies that the upper mantle under fault zones must contain relatively narrow subvertical channels through which fluids move. Actually, such channels have recently been identified from *S* wave attenuation and MTS data. Kopnichev [2000] and Kopnichev and Sokolova [2001] showed that large fault zones in Central Asia should be matched in the upper mantle by subvertical zones a few kilometers wide extending to depths of about 150 km. Rapid temporal variations in the structure of the attenuation field are observed in the Zaili fault zone at such depths [Kopnichev and Sokolova, 1997; Kopnichev, 1997, 2001]. Fluid-saturated subvertical channels ~5 km wide in the upper mantle extending to depths of up to 110 km have been identified from MTS data in the Lesser Caucasus region [Berdichevsky *et al.*, 1996].

Judging from available data, substantial variations in the structure of the fluid field can be observed not earlier than 7–10 years after earthquakes with $M > 6.5$, and the major portion of free fluids appears to leave, in some local zones, the upper mantle 30–40 years after such events. Afterward, this region of the upper mantle in the source zone remains relatively dry for a long time (possibly, a few hundred years according to data on $M \sim 7.5$ events in the Aksu earthquake zone). However,

coda characteristics in zones of coseismic paleodeformations suggest that, after a certain time interval, a new episode of fluid ascent commences in such a region. Possibly, it is the cycles related to fluid migration in the upper mantle that are responsible for the recurrence of large earthquakes in certain regions.

Figures 10 and 11 indicate that the attenuation in the upper mantle beneath the seismically passive Chu and Issyk-Kul basins is much weaker than beneath the central Tien Shan orogens. This can be regarded as evidence for a deficiency of free fluids in the lower lithosphere underlying these basins, which is consistent with the very low He isotope ratios in the water of hydrothermal springs located there [Polyak *et al.*, 1990].

Note that very weak attenuation of *S* waves in the upper mantle and, consequently, a very low fluid concentration are observed in other low-seismicity regions of Eurasia, primarily the Ukrainian Shield [Kopnichev and Pavlova, 1991]. Data on a marked difference between the characteristics of the attenuation field in seismically active and passive regions are consistent with the qualitative model of the preparation of large crustal earthquakes [Kopnichev, 1997; Kopnichev and Mikhailova, 2000], in which fluids rising from the upper mantle play an important role.

On the other hand, the results obtained in this work can be regarded as one of the physical bases for seismic regionalization. One may suppose that large earthquakes can occur where there exist, first, a high concentration of free fluids in the upper mantle responsible for strong attenuation at depths of up to 120–200 km and, second, an impermeable barrier in the middle crust characterized by very weak *S* wave attenuation and a very low electrical conductivity [Kissin, 1996; Berdichevsky *et al.*, 1996] and preventing the ascent of juvenile fluids.

Estimation of fluid field parameters in the upper mantle. Now we estimate, in a first approximation, the concentration and velocity of fluids rising in the upper mantle. Muir-Wood and King [1993] estimated at $V_f \sim 0.5$ km^3 the total volume of water that flows out onto the surface in source zones after strong ($M \sim 7.0$) crustal earthquakes. Based on our data on the very strong attenuation at depths of 20 to 50 km, we assume that this quantity is $\chi_f \sim 0.1$ of the total volume of fluids V_f rising into the crust. (Note that the parameter χ_f can significantly depend on the focal mechanism and can be much larger for normal faults than for strike-slip and reverse faults.)

Given the above estimates for an $M = 7.0$ earthquake, we assume that fluids of the total volume $V_f = 5$ km^3 rise into the crust from a region shaped as a vertical parallelepiped of length $L = 20$ km, width $W = 4$ km, and height $H = 100$ km. It is easy to see that, in this case, the volume concentration of fluids in this region is on the order of 10^{-3}.

Analysis of MTS data suggests that this quantity is an order of magnitude greater in the lower crust of tectonically active regions (10^{-2}) [Kissin, 1996]. Moreover, a high fluid concentration is apparently characteristic of the major portion of the lower crust, whereas the upper mantle fluid concentration is high only in relatively narrow subvertical zones separated by large volumes of weakly absorbing material with a negligible concentration of free fluids. Our estimate agrees with petrological ideas according to which material in the upper mantle is generally drier than in the lower crust [Ringwood, 1975].

Velocities of fluids rising in the upper mantle v_f can be estimated by using information on time shifts of steep envelope intervals (Fig. 5; Table 3).

Figure 5 shows that, in source zones of three earthquakes, high-slope intervals of coda envelopes corresponding to layers of strong attenuation in the upper mantle regularly shift with time toward lower t values. Using t_e constraints and setting the average shear velocity in the upper mantle at 4.6 km/s [Roecker *et al.*, 1993], we obtained the v_f estimates presented in Table 3.

As seen from this table, the average velocity of the fluid rising in the upper mantle beneath the source zones under consideration is a few times smaller than 1 mm/s. The v_f estimates in all source zones are similar.

Note that Table 3 gives the average fluid velocities over relatively long time intervals. Considering the upward fluid migration pattern [Fyfe *et al.*, 1978], one can assume that the fluid field front rises intermittently, so that higher interval velocities alternate with motionless periods. Moreover, by analogy with the motion of magmatic melts, the average fluid ascent velocity can be assumed to increase when the fluid approaches the Moho [Milashev, 1990].

Note for comparison that Fedotov [1976] estimated at 3–4 cm/s the average velocity of the viscous magnesian basaltic magma ascending from the base of the crust (from a depth of about 30 km) during the Great Tolbachik eruption of 1975–1976. The average velocity of kimberlite magmas rising in the crust is likely about 0.3 m/s [Milashev, 1990].

Using the data in Table 3, we can estimate the time required for fluids to completely leave a given upper mantle region. Taking $v_f = 0.3$ mm/s, we find that fluids ascend from a depth of ~220 km to the surface over

Table 3. Estimates of rising fluid velocities

Earthquake	t_e, s	v_f, mm/s	Years
Zhalanash-Tyup	85	0.2	1978
	47		1990
Baisorun	65	0.3	1990
	28		1999–2000
Suusamyr	105	0.4	1992
	70		1999

$\Delta T \sim 22$ years. Evidently, this value agrees well with the data in Fig. 9.

CONCLUSIONS

(1) The temporal variations in the structure of the *S* wave attenuation field in Tien Shan source zones of strong (M = 6.4–8.3) earthquakes were studied. The characteristics of the short-period coda were examined from aftershock records of these events, as well as from records of weak earthquakes that occurred long (up to 280 years) after the shock in question.

(2) The coda envelopes obtained from records of the first aftershocks of large earthquakes were shown to contain intervals of very steep slopes within the time interval t = 25–100 s associated with very strong attenuation of *S* waves at depths of 50 to 220 km.

(3) As the time since a strong earthquake increases, the attenuation regularly decreases at these depths and increases in the lower crust.

(4) Relatively strong attenuation in the upper mantle is observed in zones of a high density of paleofractures in the North Tien Shan produced by earthquakes with $M > 6.5$, presumably about 1000 years ago.

(5) The effects discovered in our study are interpreted in terms of mantle fluids rising into the crust through major fault zones. The fluid concentration at depths of 50 to 220 km appreciably decreases about 7–10 years after large earthquakes, and the major portion of fluids is likely to leave the upper mantle in a given zone 30–40 years after such events. Probably, a new cycle of fluid ascent begins after a certain time interval, thereby accounting for the strong *S* wave attenuation in zones of paleofractures.

(6) The fluid concentrations in the mantle roots of fault zones and the rising fluid velocities were estimated.

ACKNOWLEDGMENTS

We are grateful to S. Roecker, G.G. Shchelochkov, and B. Il'yasov for providing digital records of Tien Shan stations and to O.K. Kunakova and O.M. Shepelev for their assistance in processing the initial data.

REFERENCES

Aptikaeva, O.I. and Kopnichev, Yu.F., Space–Time Variations of the Coda Wave Envelopes of Local Earthquakes in the Region of Central Asia, *J. Earthquake Prediction. Res.*, 1993, vol. 2, no. 4, pp. 497–514.

Aptikaeva, O.I., Aptikaev, S.F., Kopnichev, Yu.F., and Rogozhin, E.A., Heterogeneities in the Lithosphere and Asthenosphere of the Turan Plate and South Tien Shan in Relation to Tectonics and Seismicity, *Fiz. Zemli,* 1996, no. 2, pp. 3–15.

Asada, T., Isibasi, K., Matsuda, T., *et al.*, *Metody prognoza zemletryasenii. Ikh primenenie v Yaponii* (Methods of Earthquake Prediction and Their Application in Japan), Moscow: Nedra, 1984.

Berdichevsky, M.N., Borisova, V.P., Golubtsova, N.S., *et al.*, Experience of the Interpretation of Sounding Data from the Lesser Caucasus, *Fiz. Zemli*, 1996, no. 4, pp. 99–117.

Curewitz, D. and Karson, J., Structural Settings of Hydrothermal Outflow: Fracture Permeability Maintained by Fault Propagation and Interaction, *J. Volcanol. Geotherm. Res.*, 1997, vol. 79, pp. 149–168.

Fedotov, S.A., On the Rise of Basic Magmas in the Crust and the Mechanism of Fissure Basalt Eruptions, *Izv. Akad. Nauk SSSR*, 1976, no. 10, pp. 5–23.

Fyfe, W., Price, N., and Thompson, A., *Fluids in the Earth's Crust*, Amsterdam: Elsevier, 1978.

Galperina, R.M., Nersesov, I.L., and Galperin, E.I., *Seismicheskii rezhim raiona goroda Alma-Aty za 1972–1982 gg.* (The Seismic Regime of the Alma-Ata Area from 1972 through 1982), Moscow: Nauka, 1985.

Italiano, F., Martinelli, G., and Nuccio, P., Anomalies of Mantle-Derived Helium during the 1997–1998 Seismic Swarm of Umbria-Marche, Italy, *Geophys. Res. Lett.*, 2001, vol. 28, no. 5, pp. 839–842.

Kaazik, P.B., Kopnichev, Yu.F., Nersesov, I.L., and Rakhmatullin, M.Kh., The Fine Structure Analysis of Short-Period Seismic Fields from a Seismic Group, *Fiz. Zemli*, 1990, no. 4, pp. 38–49.

Kissin, I.G., Fluid Saturation of the Crust, Electrical Conductivity, and Seismicity, *Fiz. Zemli*, 1996, no. 4, pp. 30–40.

Kopnichev, Yu.F., *Korotkoperiodnye seismicheskie volnovye polya* (Short-Period Seismic Wave Fields), Moscow: Nauka, 1985.

Kopnichev, Yu.F., Variations in the *S* Wave Attenuation Field Prior to Large Earthquakes in the North Tien Shan, *Dokl. Ross. Akad. Nauk*, 1997, vol. 356, no. 4, pp. 528–532.

Kopnichev, Yu.F., On the Fine Structure of the Crust and Upper Mantle at the North Tien Shan Boundary, *Dokl. Ross. Akad. Nauk*, 2000, vol. 375, no. 1, pp. 93–97.

Kopnichev, Yu.F., Long-Period Temporal Variations in the *S* Wave Attenuation Field in the Lithosphere and Asthenosphere of the North Tien Shan, *Vulkanol. Seismol.*, 2001, no. 3, pp. 63–75.

Kopnichev, Yu.F. and Nurmagambetov, A.N., Detailed Mapping of the Tien Shan Upper Mantle from the Attenuation of *S* Waves, *Fiz. Zemli*, 1987, no. 10, pp. 11–25.

Kopnichev, Yu.F. and Pavlova, O.V., Mapping of the Ukrainian Shield Upper Mantle from the Attenuation of Short-Period *S* Waves, *Vulkanol. Seismol.*, 1991, no. 3, pp. 49–58.

Kopnichev, Yu.F. and Sokolova, I.N., Variations in the Earth's Rotation Velocity and the Geodynamic Processes in Central Asia, *Dokl. Ross. Akad. Nauk*, 1997, vol. 353, no. 3, pp. 386–389.

Kopnichev, Yu.F. and Mikhailova, N.N., Geodynamic Processes in the Source Zone of the November 12, 1990, Baisorun Earthquake (North Tien Shan), *Dokl. Ross. Akad. Nauk*, 2000, vol. 373, no. 1, pp. 93–97.

Kopnichev, Yu.F., Sokolova, I.N., and Shepelev, O.M., Temporal Variations in the *S* Wave Attenuation Field in Source Zones of Large Earthquakes, *Dokl. Ross. Akad. Nauk*, 2000, vol. 374, no. 1, pp. 99–102.

Kopnichev, Yu.F. and Sokolova, I.N., Space–Time Variations in the Attenuation Field Structure of *S* Waves at the Semipal-

atinsk Test Site, *Izvestiya, Phys. Solid Earth*, 2001, vol. 37, pp. 928–941.

Krestnikov, V.N., Belousov, T.P., Ermilin, V.I., *et al.*, *Chetvertichnaya tektonika Pamira i Tyan'-Shanya* (Quaternary Tectonics of the Pamirs and Tien Shan), Moscow: Nauka, 1979.

Krestnikov, V.N., Nersesov, I.L., and Stange, D.V., The Relationship between the Deep Structure and Quaternary Tectonics of the Pamirs and Tien Shan, *Tectonophysics*, 1984.

Letnikov, F.A., *Sinergetika geologicheskikh sistem* (Synergy of Geological Systems), Novosibirsk: Nauka, 1992.

Milashev, V.A., *Kimberlity i glubinnaya geologiya* (Kimberlites and Deep Geology), Leningrad: Nedra, 1990.

Muir-Wood, R. and King, G., Hydrological Signatures of Earthquake Strain, *J. Geophys. Res.*, 1993, vol. 98, no. B12, pp. 22 035–22 068.

Nikolaev, A.V., Voitov, G.I., Grinevskii, A.O., *et al.*, Variations in Some Parameters of Water–Gas Systems in the Sartuani Mineral Water Deposit Due to the Aftershock Activity of the April 29, 1991, Racha Earthquake, *Dokl. Akad. Nauk SSSR*, 1992, vol. 326, no. 3, pp. 403–405.

Polyak, B.G., Kamenskii, I.L., Sultankhodzhaev, A.A., *et al.*, Submantle Helium in Fluids of the Southeastern Tien Shan, *Dokl. Akad. Nauk SSSR*, 1990, vol. 312, no. 3, pp. 721–725.

Ringwood, A.E., *Sostav i petrologiya mantii Zemli* (Composition and Petrology of the Earth's Mantle), Moscow: Mir, 1981.

Roecker, S., Sabitova, T.M., Vinnik, L.P., *et al.*, Three-Dimensional Elastic Wave Velocity Structure of the Western and Central Tien Shan, *J. Geophys. Res.*, 1993, vol. 98, no. 9, pp. 15 779–15 795.

Rogozhin, E.A., Tectonics of North Eurasia Source Zones of Earthquakes of the Late 20th Century, *Ross. Zh. Nauk o Zemle*, 2000, no. 2(1), pp. 37–62.

Sobolev, G.A., *Osnovy prognoza zemletryasenii* (Fundamentals of Earthquake Prediction), Moscow: Mir, 1993.

Vanyan, L.L. and Hyndman, R.D., On the Origin of the Electrical Conductivity in the Solid Crust, *Fiz. Zemli*, 1996, no. 4, pp. 5–11.

Zapol'skii, K.K., Frequency-Selective Seismic Stations, *Eksperimental'naya seismologiya* (Experimental Seismology), Moscow: Nauka, 1971, pp. 20–36.